Rev. 132, 2314 (1963), and earlier work cited therein.
[22]To test this statement, we carried out a trial phase-shift analysis wherein the Harwell $d\sigma/d\Omega$ data were deleted, and two hypothetical $d\sigma/d\Omega$ points were inserted at 10° and 20° c.m. falling on curve O [see Fig. 3(b)] with absolute accuracy ±1%. This resulted in a continuum of solutions as before, with χ^2 vs ϵ_1 nearly flat in the range $-10° \leq \epsilon_1 \leq +3°$, also as before. Thus the hypothetical data left ϵ_1 as poorly determined as ever. However, they pinned down $\delta(^1P_1)$ to a value which was nearly constant throughout the allowed range of ϵ_1. This value was $\delta(^1P_1) = -8° \pm 1°$. Thus it is possible to experimentally determine $\delta(^1P_1)$, and compare it with theory, even though ϵ_1 remains undetermined.

PHYSICAL REVIEW D VOLUME 8, NUMBER 5 1 SEPTEMBER 1973

A Statistical Measure of Clustering in Multiparticle Final States*

T. Ludlam and R. Slansky
Physics Department, Yale University, New Haven, Connecticut 06520
(Received 5 February 1973)

A quantitative measure of clustering effects in many-particle final states is defined and its significance discussed. The results consist of a single curve and a number, $\langle \omega_n{}^2 \rangle$, which may be extracted from inclusive or exclusive data where the longitudinal momenta (or some other variable) have been measured for n particles in each event. The curve is a measure of the average fluctuation of each event away from the over-all distribution, and is defined strictly in terms of experimental quantities. The results appear to provide a sensitive test for models of hadron production. Comparison with Monte Carlo calculations, or with a statistical reference model which is described, allow one to interpret the results in a fairly model-independent manner. The analysis is then applied to some 13-GeV/c K^-p data.

I. INTRODUCTION

One of the most important issues concerning multiparticle production in high-energy hadron collisions is the character of the clustering of final-state particles within the allowed phase space. The depopulation of phase space at large transverse momenta is a well-known and apparently universal signature of high-energy collision processes. However, the identification and detailed study of clustering effects in the longitudinal variables has been carried out only for specific low-multiplicity final states where exclusive analyses are feasible.[1,2] Attempts to gain more global information regarding the importance and character of clustering in the longitudinal variables have proved to be inconclusive for two reasons:

(i) The averaging inherent in measurements of inclusive cross sections appears to obscure the longitudinal clustering behavior to such a degree that models based on very different pictures of particle production are able to account equally well for much of the observed behavior of the data.

(ii) For events of high final-state multiplicity, it is difficult to make a precise operational definition of clustering. The interpretation of the longitudinal behavior is strongly colored by assumptions about the clustering effects in the transverse-momentum variables, and by the constraints imposed by energy and momentum conservation.

In this paper we recast the problem into a form which suggests a method for analyzing clustering effects in a general and model-independent manner. We analyze here some particular low-multiplicity ($n \leq 8$) data at low energy ($E \leq 30$ GeV), and point out the ease with which this analysis can be extended to the highest available energies and multiplicities.

Presently, experimental evidence for longitudinal clustering in n-body hadronic final states is obtained from studies of correlations among two or more of the $3n-4$ independent kinematic variables. Specifically, one examines a Dalitz plot, or a longitudinal phase-space plot (or prism plot),[1] or employs some other device for determining whether or not the final-state particles tend to bunch in isolated regions of the allowed phase space for some subset of the available kinematic variables.[2] An example from the class of 4-body final states for which such analyses have been carried out is $K^-p \to K^-p\pi^+\pi^-$. (See Ref. 3.) Two nearly incoherent mechanisms contribute to the final state, with each resulting in a clustering of events in separated regions of phase space. This clustering may be examined by projecting the data onto a two-dimensional plot, provided the right variables are chosen (Fig. 1). Dissociation

of the K^- beam gives rise to events with small $K\pi\pi$ effective mass and large $p\pi\pi$ mass, while target dissociation populates a region corresponding to small $p\pi\pi$ mass and large $K\pi\pi$ mass. If we had no *a priori* knowledge of the nature of the clustering effects which might be present, a plot of higher dimensionality might be required to discover this behavior.

As the multiplicity grows, the techniques for choosing revealing kinematic variables and isolating such effects necessarily becomes more complex and difficult. In general the determination of whether the final state exhibits clustering of this sort requires simultaneous examination of all $3n-4$ independent variables. For large values of n this kind of examination becomes intractable to carry out in detail. Nevertheless we take as our definition of clustering *the existence of two or more components in the final-state amplitude which add incoherently (or very nearly so) by virtue of the fact that they occupy distinct population centers of the $(3n-4)$-dimensional phase space*. Thus each event corresponds to a point in phase space, and the question of clustering concerns the structure of the population density of phase space by a large number of events. This definition is useful if it is still possible to detect the presence of different population centers when the $(3n-4)$-dimensional phase space is projected onto some smaller set of variables.

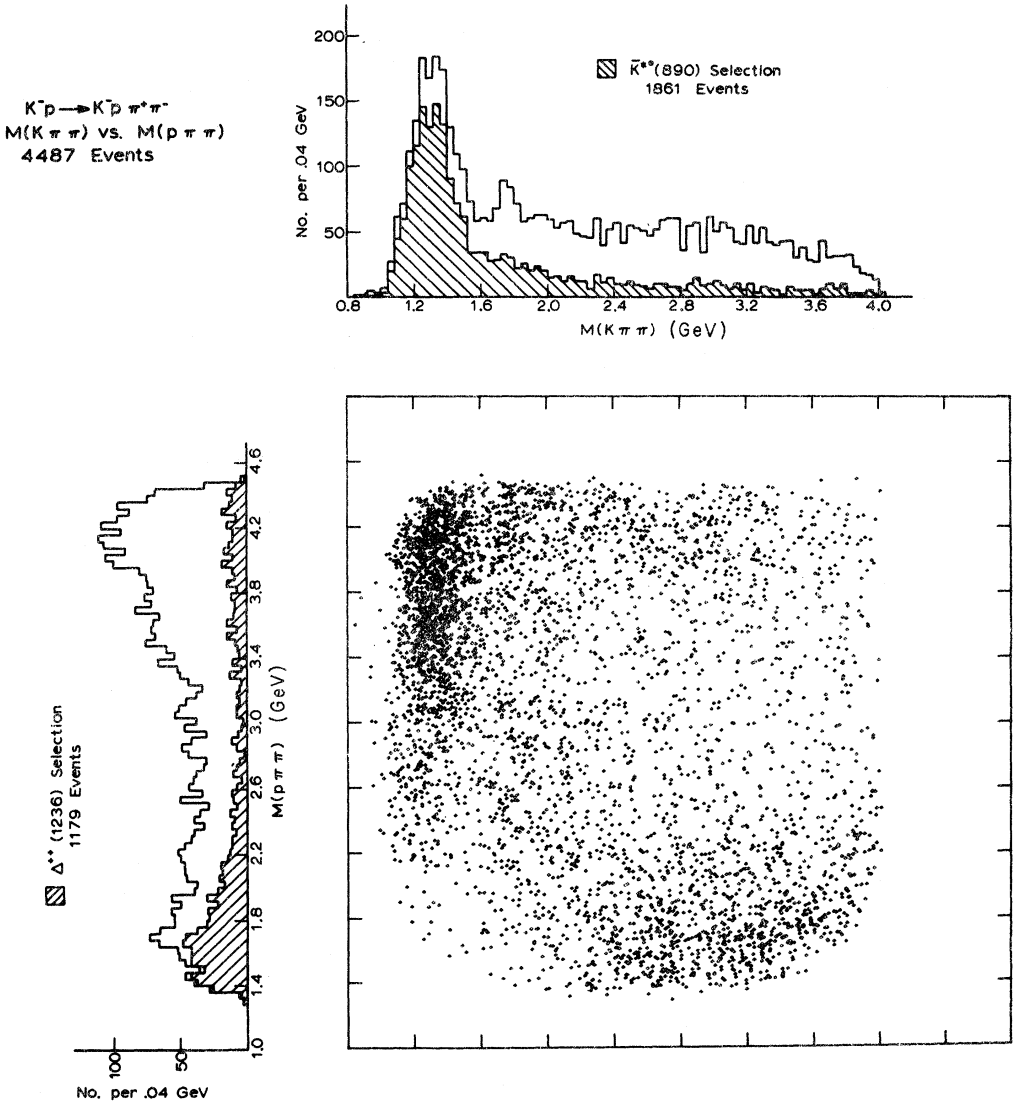

FIG. 1. Effective mass of $K^-\pi^+\pi^-$ vs effective mass of $p\pi^+\pi^-$ for the reaction $K^-p \to K^-p\pi^+\pi^-$ at 12.6-GeV/c incident beam momentum.

The procedure followed in this paper is to choose a kinematic variable, such as the longitudinal momentum or rapidity, which is measured for n particles of each event of a class of final states such as an n-body exclusive channel or n-charged-prong topological cross-section data. This set of n numbers partially defines the event point in phase space, and provides a means of projecting the single phase-space point onto n points along the axis of this variable. With a proper choice of variable, the distribution on this axis from different regions of phase space will differ. Therefore, one can obtain some information about the clustering in phase space by studying the event-to-event fluctuations about the averaged distribution in this variable.

For this purpose we propose a statistical analysis which is a direct measure of these event-to-event fluctuations, and is computed directly from the data. For exclusive channels, it provides a concise statement of the clustering properties. Inclusively, it provides new information not directly manifested in the one- and two-particle distributions. It can also be computed from models and should be a serious challenge to models committed to a specific pattern of clustering.

Consider a set of N events where, for each event, n longitudinal variables are measured. This could be, for example, the lab momenta or $\eta = -\ln(\tan\frac{1}{2}\theta)$ values of the n charged tracks in the n-prong topological cross-section data, or it could be the rapidities of the n final particles (or some subset of particles) in a specific exclusive final state. The distribution of these nN numbers (we shall call them rapidities for definiteness) is $p(y)$, where $p(y)\Delta y$ is the fraction of the nN rapidities which fall between $y-\frac{1}{2}\Delta y$ and $y+\frac{1}{2}\Delta y$. This average distribution (averaged over the N events) provides an unambiguous and model-independent reference to which a clustering measure may be defined. The analysis is designed to answer the question, does *each* event produce a set of n rapidities which follow $p(y)$? We construct a quantitative measure of the average event-to-event fluctuations which can be easily compared with the random statistical fluctuations which would result if every event followed $p(y)$.

With the aid of a simple example, it is easy to see how such a fluctuation measure can shed light on the question of clustering and why a statistical analysis is necessary. Consider the problem of discriminating between two general pictures of particle production. In the short-range order picture, the presence of a particle with a given value of $y = y_0$ does not affect the probability of finding other particles at values of y far from y_0. Then, to a good approximation, each event follows $p(y)$, and the fluctuations will be mainly statistical. This leads to the same fluctuation results as found in multiperipheral models which are characterized by secondaries which tend to be uniformly spaced in rapidity. Again, the event-to-event fluctuations will be small. This should be contrasted with models which view particle production as the decay of massive states. Then many of the secondaries would appear in a region narrower than $p(y)$, if several such mechanisms are present. An extreme example is a sample in which some events proceed by beam excitation, and others by target excitation. This would give rise to large fluctuations, since the distribution of beam or target excitation by itself differs from the averaged distribution, at least for some choices of the projection variable.

The need for a *statistical* analysis can be seen from an extreme fragmentation model. Suppose particle production proceeds by the formation of massive objects whose "decay" distributions are isotropic in the object's rest frame. The requirement that the decay distribution be consistent with the experimentally observed transverse momentum behavior implies that the full width at half maximum of its distribution is from 2 to 2.5 units of rapidity. Of course, it is easy to imagine distributions which are wider in rapidity, say, due to polarization effects. But this value is already close to the width of the pion rapidity distributions for $E_{\text{lab}} \leq 30$ GeV, and to the width of the high-multiplicity semi-inclusive distributions observed at very high energies. Thus, if several mechanisms are present, even if they are well separated in the $(3n-4)$-dimensional phase space, the contributions to $p(y)$ are expected to overlap. Therefore, it is impossible from the rapidity distribution to assign a mechanism to each event (assuming that several exist), but it is still possible to use a statistical measure to detect their existence. It should become intuitively clear that such a fluctuation measure is more sensitive to clustering than to short-range correlations.

In Sec. II, we proceed directly to the definition and computation of the fluctuations. Then we compare the analysis with some techniques of "distribution-free" statistics, discuss the effect of energy-momentum conservation, and outline a statistical reference model with which to compare the data. The details of the reference model are included in the Appendix.

In Sec. III, we return to the problem of interpreting the results of the analysis, and explicitly study some 13 GeV/c K^-p data.[3] Applications are given to both inclusive and exclusive reactions.

The results of the analysis are summarized in Sec. IV.

II. EXPERIMENTAL DETERMINATION

In the Introduction, we defined clustering in terms of the existence of distinct population centers in the full phase space of an n-body final state. We now describe a statistical analysis for clustering which involves studying the fluctuations of the distribution of rapidities of each event about the average distribution.

Consider again a data sample of N events, where n rapidities (or other kinematic variables) are measured in each event. The distribution density is denoted by $p(y)$, and the cumulative distribution function is defined by

$$F(y)=\int_{-\infty}^{y} dy' p(y'), \tag{1}$$

where $F(-\infty)=0$ and $F(+\infty)=1$. A convenient measure of the fluctuation of the distribution of event i $(i=1, \ldots, N)$ is based on the quantity

$$\mu_i(y)=[S_{n,i}(y)-F(y)]^2 p(y). \tag{2}$$

$F(y)$ and $p(y)$ are average distributions obtained from the entire sample of N events. The empirical distribution function, $S_{n,i}(y)$, is defined for each event:

$$S_{n,i}(y)=\frac{r}{n} \quad (i=1, \ldots, N), \tag{3}$$

if in the ith event there are r particles with rapidities less than or equal to y, and consequently $n-r$ particles with rapidities greater than y. $S_{n,i}(y)$ is a step function with n steps of height $1/n$ at each of the rapidities. Thus, the average of the empirical distribution function over the N events is

$$\frac{1}{N}\sum_{i=1}^{N} S_{n,i}(y) \equiv \langle S_n(y)\rangle = F(y), \tag{4}$$

where $\langle \cdots \rangle$ in this paper means "average over the sample of N events." Equation (4) is just the experimental definition of $F(y)$.

Two important quantities may be defined from Eq. (2). The first is the average *fluctuation density*

$$M(y)=\langle [S_n(y)-F(y)]^2\rangle p(y)$$
$$=[\langle S_n(y)^2\rangle - \langle S_n(y)\rangle^2]p(y). \tag{5}$$

$M(y)$ is the average fluctuation of the empirical distribution function away from the average cumulative distribution weighted by $p(y)$. The choice of this combination of factors is discussed below. The second quantity is the statistic[4]

$$\omega_{n,i}{}^2=\int dy\, \mu_i(y), \quad i=1, \ldots, N \tag{6}$$

which can be calculated for each event. The average of $\omega_n{}^2$ is related to $M(y)$ by

$$\langle \omega_n{}^2\rangle = \int dy\, M(y). \tag{7}$$

We found the first moment of the $\omega_n{}^2$ distribution to be the most useful.

The experimental determination of $M(y)$, $p(y)$, and $\langle \omega_n{}^2\rangle$ can easily be done with a single pass through the data. Given the values of the n rapidities (or other variables) for the event, accumulate bin by bin the averages $\langle S_n(y)\rangle$, $p(y)$, and $\langle S_n(y)^2\rangle$. As discussed below, it is sometimes useful to accumulate the distribution of the sum of the y's for each event. We call this distribution $\rho(z)$, where z is computed for each event:

$$z=\sum_{i=1}^{n} y_i. \tag{8}$$

(For example, in an exclusive reaction where y is the longitudinal momentum, $\rho(z)$ is a δ function.) Finally, evaluate $M(y)$ and $\langle \omega_n{}^2\rangle$ according to Eqs. (5) and (7).

Formally, $\omega_n{}^2$ in Eq. (6) is identical to the Cramér-von Mises[4] statistic, which can be applied to goodness-of-fit problems in a way similar to the χ^2 test. The Cramér test possesses some very nice properties.[4,5] Suppose n independent random rapidities are generated, each following a probability density $p(y)$ with cumulative distribution $F(y)$. Then the distribution function of $\omega_n{}^2$ does *not* depend on $p(y)$, i.e., it is distribution free. Thus, $\langle \omega_n{}^2\rangle$ also does not depend on $p(y)$, and, as shown in the Appendix, $\langle \omega_n{}^2\rangle = 1/6n$. In the case where the n independent rapidities are generated by one of a sum of different distributions which average out to $p(y)$, the fluctuations are larger on the average, and $\langle \omega_n{}^2\rangle > 1/6n$. Then $\langle \omega_n{}^2\rangle$ would be a measure of the difference of these distributions from the over-all distribution, and the reference value $\langle \omega_n{}^2\rangle = 1/6n$ would provide a model-independent reference with which to compare the data.

Unfortunately, the statistical independence of the n rapidities is a crucial assumption in the Cramér test, whereas the rapidities in both exclusive and inclusive final states are strongly constrained by energy-momentum conservation. Even in the case of a single population center in phase space, $\langle \omega_n{}^2\rangle$ is no longer distribution-free, but depends on the effectiveness of these constraints and the shape of $p(y)$. In order to conserve momentum and energy, the rapidities are spaced out over the $p(y)$ distribution in such a way that the fluctuations are smaller than obtained for a truly random sample. In exclusive final states analyzed in terms of longitudinal momentum, the numerical

value $\langle\omega_n^2\rangle$ is reduced to about 1/2 the $1/6n$ value.

The most direct way of incorporating energy-momentum conservation is to perform Monte Carlo simulations, compute $M(y)$ and $\langle\omega_n^2\rangle$, and then compare with the data. The requirement for such a reference calculation is that the y_i for each event follow the same probability distribution, subject, of course, to the constraints of energy-momentum conservation.

The dependence of $\langle\omega_n^2\rangle$ on the shape of $p(y)$ is rather weak, so an accurate fit to $p(y)$ is not needed. It therefore proves possible to define an accurate reference value for $\langle\omega_n^2\rangle$ which represents no clustering, but in which energy-momentum conservation effects are accounted for, and $\langle\omega_n^2\rangle$ is still sensitive to more interesting clustering effects. (Short-range correlation effects contribute very little to $\langle\omega_n^2\rangle$.) Thus, in practice it is possible to regain the elegance and power of the Cramér test. With the new advances in event generation techniques,[6] it is quite simple to apply this procedure up to the highest experimentally accessible energies and multiplicities.

We have found that a second technique for obtaining reference values for $\langle\omega_n^2\rangle$ is also useful. This is a statistical model in which the constraints are approximately imposed. The model described here is the simplest in a class of models, and it will be clear that generalizations and modifications are possible.

The idea behind the analytic model is to use the data for $\rho(z)$ [$\rho(z)$ is the distribution of the sum of rapidities defined in Eq. (8)] to define the constraint. In the statistically-independent (Cramér) case, $\rho(z)$ is an n-fold convolution of $p(y)$. For exclusive reactions where y is the longitudinal momentum, $\rho(z)$ is a δ function. With this constraint, longitudinal momentum conservation is exactly accounted for, but energy conservation is ignored. The effects of energy conservation sometimes further decrease $\langle\omega_n^2\rangle$ by as much as 10%. For other longitudinal variables, and in inclusive reactions, $\rho(z)$ will be some distribution which measures the effectiveness of energy-momentum conservation in constraining the rapidities. In this simple model we do not include the second constraint. Moreover, if several mechanisms are present and a variable like rapidity or $-\ln(\tan\frac{1}{2}\theta)$ is used, $\rho(z)$ may be broadened over that required by energy-momentum conservation. This will artificially increase the reference value for $\langle\omega_n^2\rangle$. For this reason, this model only gives an upper limit for the no-clustering value of $\langle\omega_n^2\rangle$. In detailed analysis of data we have found the Monte Carlo technique for obtaining a precise value of the statistical reference to be essential. The analytic model does, however, provide useful insights into the analysis. The details are included in the Appendix, and one solution to the model is presented in Table I. In this case, $p(y)$ is a Gaussian with standard deviation σ_y, and $\rho(z)$ is also a Gaussian of standard deviation σ_z. Then $\langle\omega_n^2\rangle$ depends on n and $r=\sigma_z/\sigma_y$. When $r=\sqrt{n}$, the Cramér limit is recovered. Table I gives $\langle\omega_n^2\rangle$ as a function of r and n.

III. INTERPRETATION OF $M(y)$—A STUDY OF SOME 13-GeV/c K^-p DATA

A. Exclusive Four-Body Final States

The fluctuation analysis is appropriate for detecting clustering from projections of the $(3n-4)$-dimensional phase space. For a good choice of variable, the distributions projected from different mechanisms will be different, even though they are expected to overlap. The advantage of the fluctuation analysis is that one can test for the presence of overlapping distributions without assigning a specific mechanism for each event. Thus, to a degree, the difficulties of a complete multidimensional phase-space analysis are avoided.

We now apply the fluctuation analysis to two exclusive channels[3]

$$K^-p \to K^-p\pi^+\pi^-, \tag{9}$$

$$K^-p \to \overline{K}^0p\pi^0\pi^- \tag{10}$$

at 12.6 GeV/c. Our analysis here is intended to show how the fluctuation analysis works in some channels which are well understood on the basis of previous analyses.

The mass scatter plots in Figs. 1 and 2 already indicate the general structure of phase space for these reactions. In reaction (9) the $K^-p\pi^+\pi^-$ final state presents two well-separated components

TABLE I. Gaussian reference values for $\langle\omega_n^2\rangle$. r is the ratio of the standard deviation of $\rho(z)$ to the standard deviation of $p(y)$, n is the number of measured tracks. See the Appendix for the derivation of the Gaussian reference. The table entries are $1000\times\langle\omega_n^2\rangle$.

	$r/\sqrt{n}$					
n	0	0.2	0.4	0.6	0.8	1.0
3	26.8	27.9	31.2	36.8	44.8	55.6
4	19.7	20.6	23.1	27.4	33.5	41.2
5	15.6	16.3	18.4	21.9	26.8	33.3
6	12.9	13.5	15.2	18.2	22.3	27.8
8	9.60	10.0	11.4	13.6	16.7	20.8
10	7.64	7.99	9.06	10.8	13.4	16.7
12	6.34	6.64	7.54	9.03	11.1	13.9
14	5.42	5.68	6.45	7.74	9.55	11.9
16	4.74	4.96	5.64	6.77	8.36	10.4

corresponding to diffractive excitation of either the beam or the target particle. The former is characterized by a low-mass enhancement in the $K\pi\pi$ invariant mass (the Q "meson") and the latter by a similar enhancement near threshold in the $p\pi\pi$ invariant mass. As seen in Fig. 1, little overlap occurs between these two components. This is apparently a two-mechanism case, satisfying the definition of clustering given above. In reaction (10) (Fig. 2), only one of these components is observed (here the $p\pi\pi$ system cannot be produced by the exchange of vacuum quantum numbers). This, to a good approximation, is a single-mechanism, or no-clustering case, and these two reactions should offer an excellent laboratory for testing the ideas outlined in Sec. II. They are characteristic of (but not necessarily identical to) the kinds of effects one would like to be able to recognize in more complicated final states.

We point out that several different amplitudes may be contributing to each of the final-state components which we have just described. Thus the Dalitz plot for the low-mass $K\pi\pi$ enhancement in both reactions (9) and (10) is composed of overlapping bands of $K^*(890)\pi$ and $K\rho$. These, however, are highly coherent. They do not populate isolated regions of phase space. In our language they constitute short-range correlations and do not contribute separately to the clustering content of these two reactions.

In Figs. 3 and 4 we compare the distributions $p(y)$ and $M(y)$ for the reactions (9) and (10) with one-mechanism Monte Carlo calculations. Here we choose as our variable the longitudinal momentum in the c.m. frame: $y = k_L^{c.m.}$. The purpose of the Monte Carlo calculations is to provide a reference in which the fluctuations are purely statistical, but in which energy and momentum are conserved.

As we have discussed above, the effect of ener-

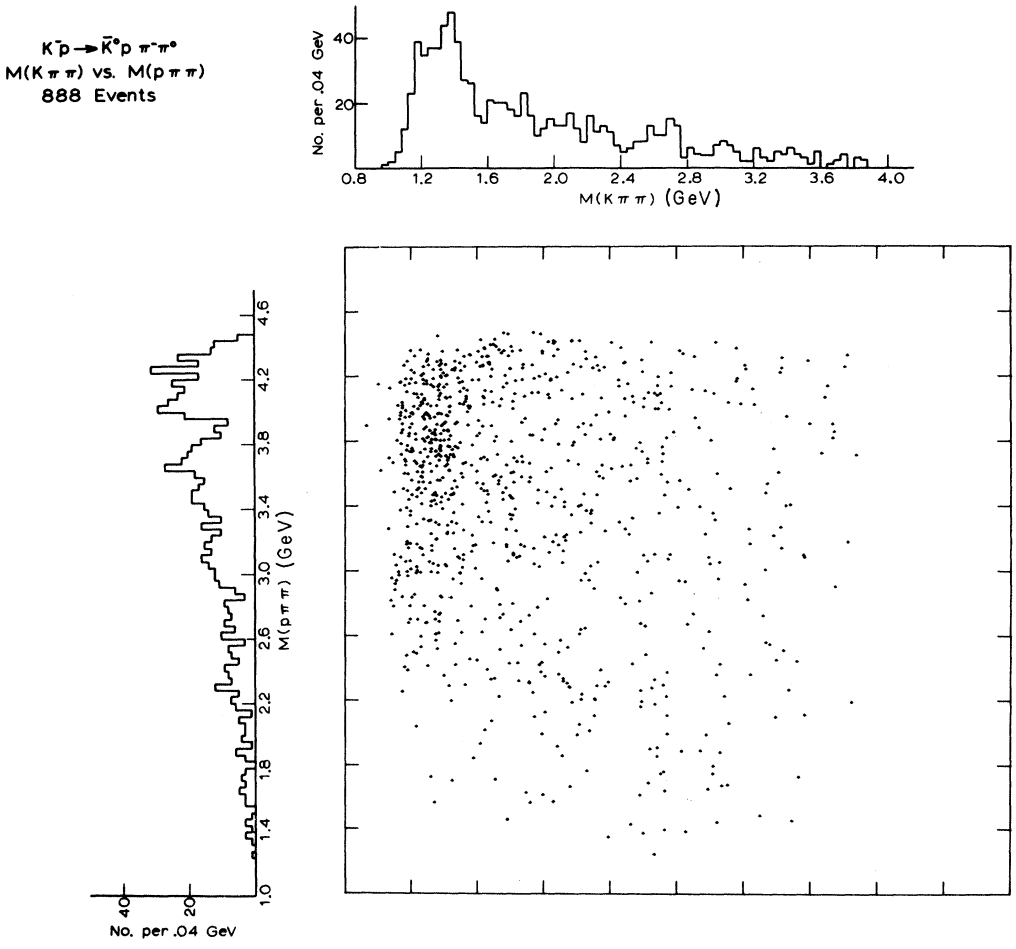

FIG. 2. Effective mass of $\bar{K}^0\pi^-\pi^0$ vs effective mass of $p\pi^-\pi^0$ for the reaction $K^-p \to \bar{K}^0 p\pi^-\pi^0$ at 12.6-GeV/c incident beam momentum.

gy-momentum conservation is to reduce the reference value of $\langle\omega_n^2\rangle$ by about a factor of 2 from the distribution-free value of $1/6n$ obtained if the constraints are not present. When the constraints are imposed, it is not mathematically true that $\langle\omega_n^2\rangle$ continues to be a distribution-free quantity. However, the great convenience of this measure of clustering is that, for a given reaction and choice of y, the reference value of $\langle\omega_n^2\rangle$ is very nearly independent of the shape of $p(y)$. The only reason to reproduce the data is to compare the reference curves for $M(y)$ with the data in order to see where the fluctuations are largest. No attempt need be made to fit $p(y)$ in detail. In every case shown here, the reference value of $\langle\omega_n^2\rangle$ differs by less than 2% from that obtained simply from events distributed according to Lorentz-invariant phase space with transverse-momentum dependence $\exp(-3k_T^2)$ on all final-state particles.

The fake data for comparison with reaction (9) were obtained by modifying Lorentz-invariant phase space with exponential cutoffs in the transverse momenta of each of the mesons $\sim\exp(-3k_T^2)$, and a similar cutoff on the proton-to-proton momentum transfer $\sim\exp(3t_{pp})$. In the case of reaction (10), we achieved an adequate fake representation of $p(y)$ with a single multiperipheral diagram involving Pomeranchuk exchange at the proton vertex.

For reaction (9) (Fig. 3) the value $\langle\omega_n^2\rangle$ for the data is appreciably larger than for the fake: 0.0172 compared with 0.0143. The errors on these numbers are much less than 1%.[7] Referring to Fig. 3(a), it can be seen from the $M(y)$ distributions that the larger value of $\langle\omega_n^2\rangle$ in the data is due to fluctuations which are significantly greater than the statistical case for $k_L^{c.m.}$ near zero. [Recall that $\langle\omega_n^2\rangle$ is the area under the curve $M(y)$.] This is, in fact, the region in which comparatively large fluctuations are expected in this two-mechanism example. The produced pions are almost always slow in the c.m. frame, and it is here that the two population centers, corresponding to beam and target excitation, overlap when projected onto the $k_L^{c.m.}$ axis. In contrast with this result, the fluctuation density $M(y)$ for reaction (10) [Fig. 4(a)], which we have described as a single-mechanism case, is only slightly above the reference value,

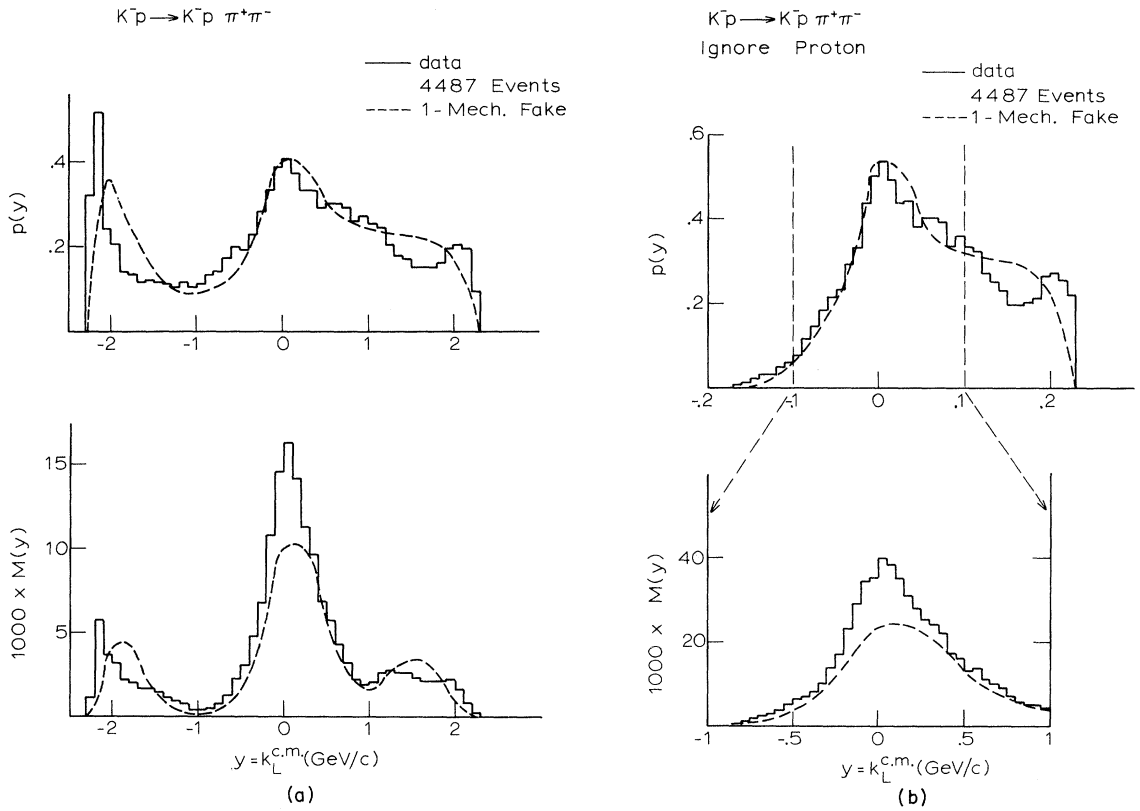

FIG. 3. Fluctuation analysis for $K^-p \to K^-p\pi^+\pi^-$ at 12.6 GeV/c. The histograms are the distributions $p(y)$ and $M(y)$ for the data, and the smooth curves are the results of the analysis applied to the single-mechanism model described in the text. In Fig. 3(a), all four final-state particles are included in the analysis, while in Fig. 3(b), the final-state proton is ignored. Note the expanded horizontal scale for the $M(y)$ distribution in Fig. 3(b).

which reflects the dominance of beam excitation. Note that the strong peaking seen in Fig. 3 of $M(y)$ at $k_L^{c.m.} \approx 0$ is absent in this case.

In both reactions (9) and (10) the proton distribution is strongly peaked in the backward direction regardless of the production mechanism. The proton contributes very little to the enhanced fluctuations above statistics in reaction (9). Thus it is of interest to carry out the analysis ignoring the proton in each event—examining only the fluctuations due to the meson distributions. The results are shown in Figs. 3(b) and 4(b). The relative values of the $M(y)$ and their respective references are essentially unchanged, but the sensitivity of $\langle \omega_n^2 \rangle$ to the clustering in reaction (9) is greatly increased. This is simply because the proton contributes only statistical fluctuations to $\langle \omega_n^2 \rangle$. Again, the value of $\langle \omega_n^2 \rangle$ for reaction (10) indicates little clustering when compared with the reference calculation.

We conclude that the analysis in terms of $\langle \omega_n^2 \rangle$ and $M(y)$ is adequately sensitive to the known clustering content of these two 4-body channels, and that this sensitivity is not diluted by the presence of contributions due to various forms of 2-body resonance production (i.e., short-range correlations). Our hope, of course, is to be able to apply this analysis to more complicated situations with meaningful results. In the remainder of this section, we investigate its sensitivity to clustering in events of higher multiplicity, including the case in which the final states are not fully identified (inclusive data).

The values for $\langle \omega_n^2 \rangle$ from the exclusive data and various model calculations are summarized in Table II.

B. $K^-p \to K^-p\pi^+\pi^-\pi^0$

When one is confronted with an 11-dimensional phase space, it is not obvious which projections of the data to study. Because of its success in the four-body analysis, we show the scattergram of the $K^-\pi^+\pi^-\pi^0$ vs $p\pi^+\pi^-\pi^0$ invariant masses in Fig. 5. There is no clear separation like that observed in Fig. 1, but the uniform $K^-\pi^+\pi^-\pi^0$ mass distribution

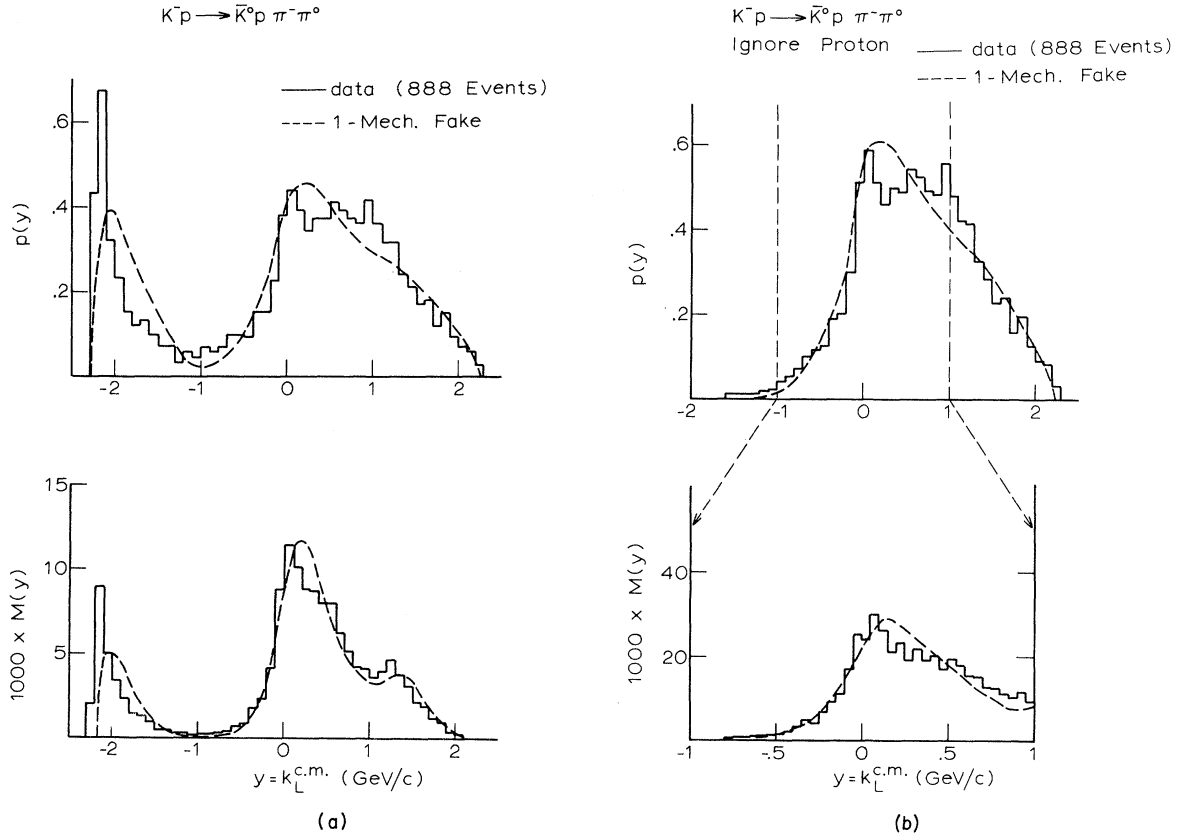

FIG. 4. Fluctuation analysis for $K^-p \to \bar{K}^0 p \pi^-\pi^0$, at 12.6 GeV/$c$. The data are histogrammed. The single-mechanism model, described in the text, gives the smooth curves. In Fig. 4(a) all four final-state particles are included in the analysis, and in Fig. 4(b) the proton is ignored. The horizontal scale for $M(y)$ is expanded in Fig. 4(b).

could be due to the overlap of several mechanisms. If there is clustering in this reaction, Fig. 5 does not prove it.

We begin by applying the fluctuation analysis to two model calculations for this final state. The first is a single-mechanism model where the p and K^- spectra are generated with the distributions $\exp(3t_{pp})$ and $\exp(3t_{KK})$, respectively, and the pion distributions are all generated with $\exp(-3k_T^2)$. This is a typical one-mechanism reference model, and the result, $\langle\omega_n^2\rangle = 0.0121$, is quite insensitive to changes of details. The second model is a fragmentation picture where half of the events correspond to beam fragmentation, and the other half to target fragmentation. The contributions of each of these mechanisms to $p(y)$ are shown in Fig. 6, where it is seen that the beam and target excitation distributions strongly overlap when projected on $k_L^{\text{c.m.}}$. But the difference is enough to give a size-

TABLE II. Values for $\langle\omega_n^2\rangle$: exclusive analyses of 12.6-GeV/c K^-p final states. The model calculations are described in Secs. III A and III B. The one-mechanism reference model results are given immediately below the experimental data.

	All	Ignore proton
$K^-p\pi^+\pi^-$	0.0172	0.0351
Model	0.0143	0.0276
$\bar{K}^0p\pi^0\pi^-$	0.0147	0.0295
Model	0.0143	0.0277
$K^-p\pi^+\pi^-\pi^0$	0.0154	0.0290
Model	0.0121	0.0210
Two-mechanism model	0.0158	0.0305

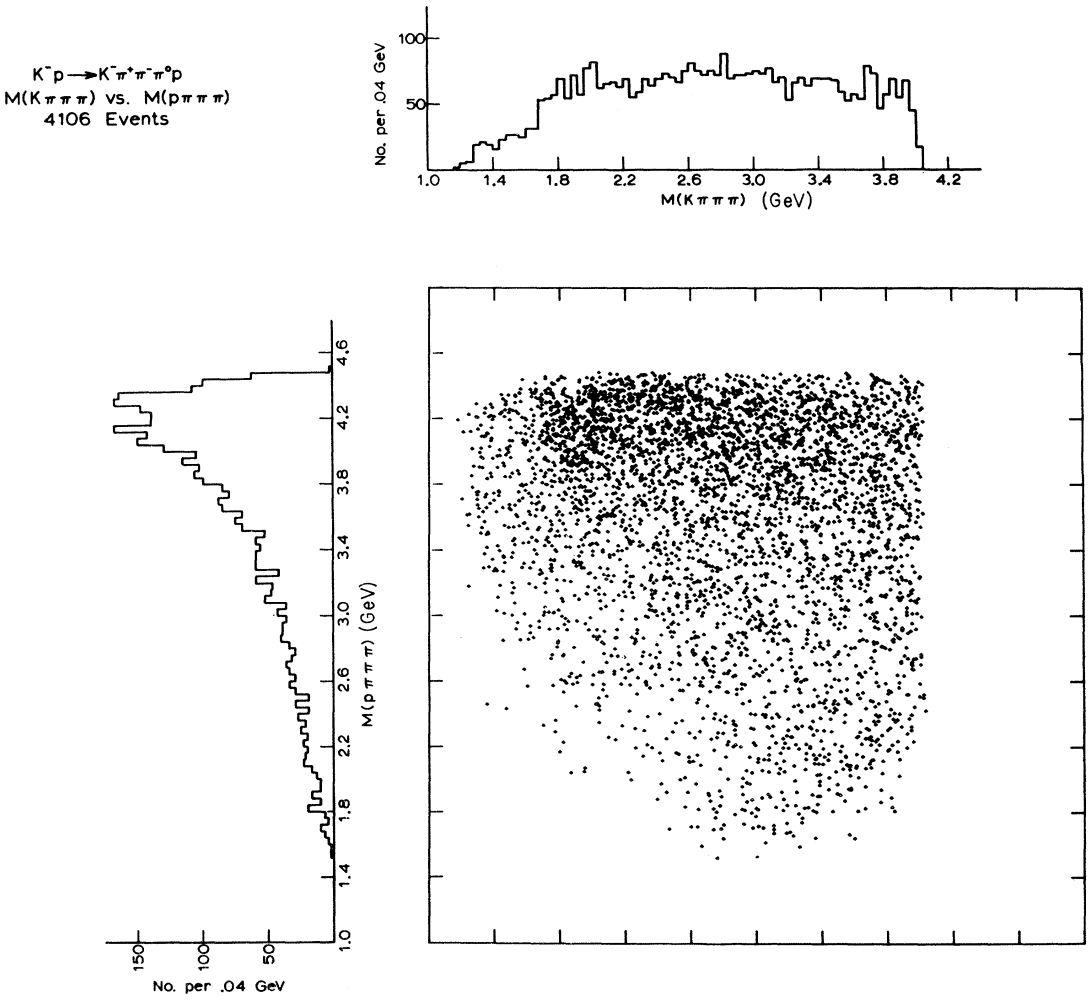

FIG. 5. The $K\pi\pi\pi$ effective mass plotted vs $p\pi\pi\pi$ effective mass for the reaction $K^-p \to K^-p\pi^+\pi^-\pi^0$ at 12.6 GeV/c.

able increase in the fluctuations, and $\langle\omega_n{}^2\rangle = 0.0158$ for this two-mechanism model. The distributions $p(y)$ and $M(y)$ for these two models are shown in Fig. 7(a). Just as in the four-body reactions, the $M(y)$ curves are essentially identical except near $k_L^{\text{c.m.}} \approx 0$, where the fluctuations are greatly enhanced in the two-mechanism case. The analysis of these two models is repeated in Fig. 7(b) ignoring the proton. Again, the fluctuations become more obvious because the clustering effects are reflected mainly in the meson distributions.

In Fig. 8, the data for this 5-body final state are compared with the single-mechanism Monte Carlo model. See Table II for the values of $\langle\omega_n{}^2\rangle$. Although the mass scattergram in Fig. 5 is not conclusive, the fluctuation analysis shows that this final state is strongly clustered. Detailed examination of this final state by more conventional techniques reveals the presence of several very different production mechanisms which contribute to the observed fluctuations in this channel.[1] For practical reasons these more differential analyses

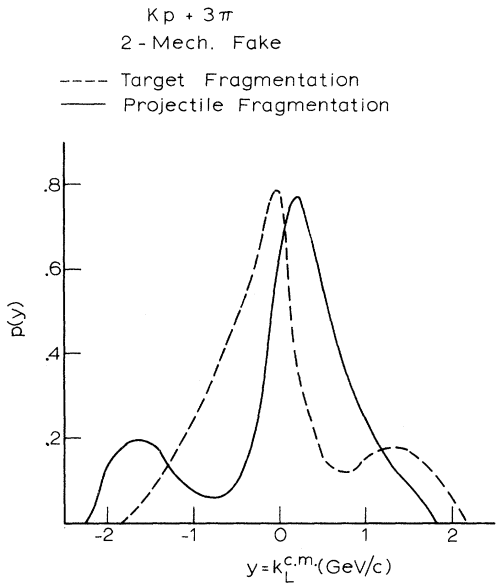

FIG. 6. Contributions of beam and target excitation to the distribution $p(k_L^{\text{c.m.}})$ in the two-component model for $Kp \to Kp + 3\pi$.

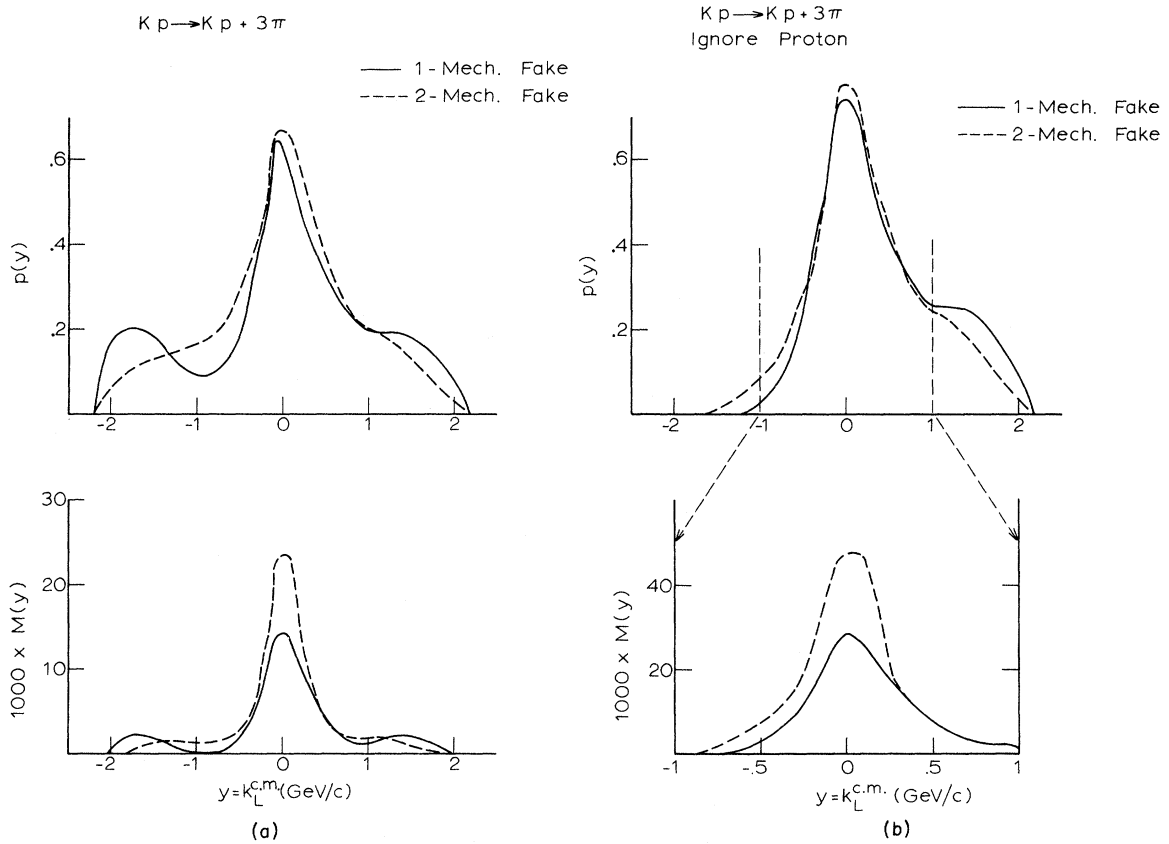

FIG. 7. Fluctuation analysis applied to models for $Kp \to Kp3\pi$. The solid curves correspond to the one-mechanism model, and the dashed curves to the two-mechanism model. In Fig. 7(a), all 5 final particles are analyzed, and in Fig. 7(b) the proton is ignored. See Sec. III B for a description of the models. In Fig. 7(b) the horizontal scale for $M(y)$ is expanded.

are limited to relatively small multiplicities. However the fluctuation analysis can be used to *detect* such behavior in a simple and straightforward way. Furthermore, it appears to gain in sensitivity as the multiplicity is increased without any additional practical complication.

C. Inclusive Analyses

The main requirement of a variable for the analysis is that projections of different population centers of phase space produce slightly different distributions. Thus, $\eta = -\ln(\tan\frac{1}{2}\theta)$ and $k_L^{\rm lab}$ are expected to be good variables for studying longitudinal clustering. Since particle identification is not necessary for evaluating these variables, fluctuation analyses on topological cross-section data are possible.

An inclusive analysis involves projecting phase-space volumes of different dimensions onto the η (or $k_L^{\rm lab}$) axis. *A priori*, it is difficult to know whether such a projection will wash out the fluctuations due to clustering. As a preliminary step in the inclusive analysis, we add together the data for the $K^-p\pi^+\pi^-$ and $K^-p\pi^+\pi^-\pi^0$ final states, ignoring the π^0 in the latter case. We also ignore the fact that the particle identities are known here, taking η as our projection variable ($y=\eta$, and θ is defined in the laboratory frame). These two channels together make up about 15% of the 4-prong data in 13-GeV/c K^-p collisions. Both have strong clustering, although the patterns differ in these two channels, and of course, the two channels have different multiplicities of final-state particles. In Fig. 9 we have compared the summed data for these two channels to a similar sum made up from the one-mechanism Monte Carlo reference calculations shown in Figs. 3 and 8. An examination of the $M(y)$ curves shows that the clustering analysis is still effective. The values of $\langle\omega_n^2\rangle$ for data and reference are 0.0248 and 0.0204, respectively.

The values of $\langle\omega_n^2\rangle$ for the 4-, 6-, and 8-prong K^-p data are listed in Table III. The analyses were done in terms of $\eta^{\rm lab}$. The reference values for the n-prong values of $\langle\omega_n^2\rangle$ were obtained from Monte Carlo events with an $\exp(-3k_T^2)$ dependence for each secondary. Events with multiplicities

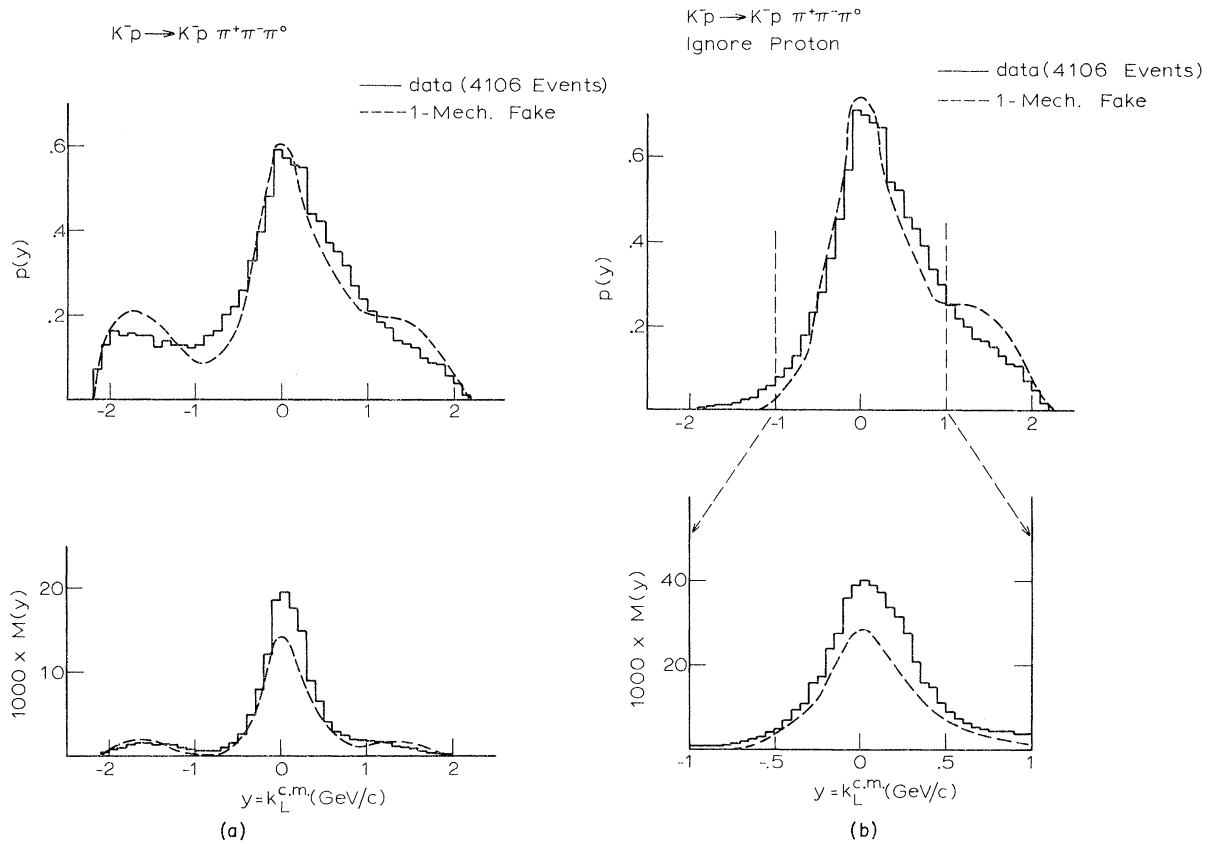

FIG. 8. Fluctuation analysis for $K^-p \to K^-p\pi^+\pi^-\pi^0$ at 12.6 GeV/c. The data are histogrammed, the single-mechanism model described in the text gives the solid curve. In Fig. 8(a), all 5 final particles are included in the analysis, and in Fig. 8(b) the proton is ignored. Note the expanded horizontal scale for $M(y)$ in Fig. 8(b).

n, $n+1$, $n+2$, ... were generated according to the experimentally observed charged-particle multiplicity distribution. In each event, the fluctuation analysis was applied to only n of the final-state particles. This estimate for the multiplicity distribution at fixed charged multiplicity may not contain enough neutral production. This introduces an uncertainty in the reference value of about 20%.

The values of $\langle\omega_n{}^2\rangle$ for the topological cross-section data are significantly larger than the corresponding reference values. This is also true for the 8-prong data, which is high-multiplicity for this energy. It appears, then, that the large fluctuations seen in the exclusive channels may be characteristic of a large fraction of the inelastic K^-p cross section at these energies.

The Gaussian reference shown in Table III is, in all cases, significantly larger than the true reference values. We include this result to emphasize that the Gaussian reference is only an upper limit, and that Monte Carlo calculations are necessary for a correct comparison with the data.

We conclude this section with some comments on other approaches to the constraint problem. Although the energy-momentum constraints do not cause any difficulties in principle, one still might attempt to define a new longitudinal variable in which the conservation laws somehow "factor out", and only the clustering contributions are left. We were unable to find such a variable. Several other ideas for avoiding the constraint simply fail. If only one particle is chosen per event [$S_1(y)$, a simple θ function], then the fluctuations are so large that the most obvious clustering effects are washed out. This much is obvious. But there is a variant which runs into the same difficulty. This is to apply the test to the rth order statistic generated by $p(y)$. Here again, the statistical fluctuations overwhelm any clustering contributions. Although it may prove possible to avoid the constraint problem altogether, we found it quite feasible to confront it directly.

IV. SUMMARY

We have defined clustering in hadronic final states as the existence of two or more population centers in phase space, and shown that fluctuations

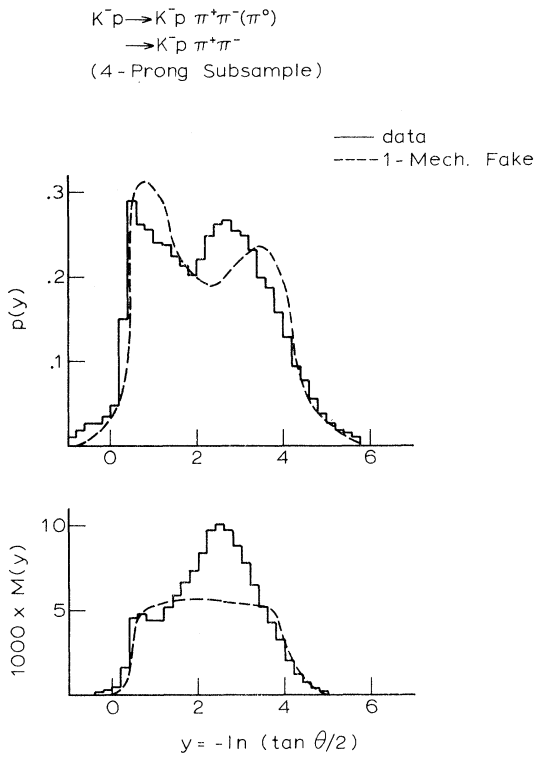

FIG. 9. Application of fluctuation analysis to the sum of the $K^-p\pi^+\pi^-$ and $K^-p\pi^+\pi^-\pi^0$ data (π^0 ignored). The data are plotted in terms of $\eta=-\ln(\tan\frac{1}{2}\theta^{\rm lab})$, and compared to the sum of the single-mechanism Monte Carlo models for these final states.

about the projected distribution $p(y)$ are large enough in practical situations for this clustering to be detected by a statistical analysis involving only a single kinematic variable. This fluctuation analysis may be applied to inclusive as well as exclusive data, and becomes more sensitive as the multiplicity of final-state particles increases, with no additional practical complications. We have applied the analysis to some 13-GeV/c K^-p data with the following results:

(a) The known differences in the clustering behavior of the 4-body reactions

$$K^-p\to K^-p\pi^+\pi^-$$

and

TABLE III. Inclusive analysis of 12.6-GeV/c K^-p final states. The reference calculation is described in Sec. III C. The projection variable is $\eta=-\ln(\tan\frac{1}{2}\theta^{\rm lab})$.

Topology	No. events	$\langle\omega_n{}^2\rangle$ data	$\langle\omega_n{}^2\rangle$ reference	$r=\sigma_z/\sigma_y$	Gaussian reference
4-pr	23 990	0.0347	0.0235	1.61	0.0337
6-pr	5470	0.0232	0.0162	2.04	0.0231
8-pr	848	0.0168	0.0133	2.25	0.0167

$K^-p \to \overline{K}^0 p\pi^-\pi^0$

are readily distinguished.

(b) Strong clustering is observed in the 5-body final state resulting from $K^-p \to K^-p\pi^+\pi^-\pi^0$.

(c) The data for $K^-p \to K^-p\pi^+\pi^-$ and $K^-p \to K^-p\pi^+\pi^-\pi^0$ were combined, ignoring the π^0 in the latter case and performing the analysis in terms of the variable $\eta = -\ln\tan\frac{1}{2}\theta$ (i.e., ignoring all particle identification). The effects of clustering were still in evidence in the statistical analysis. Thus inclusive analysis on topological cross-section data is feasible. For these analyses, a no-clustering reference must be obtained from Monte Carlo calculations.

(d) The 4-, 6-, and 8-prong inclusive data samples all appear to show fluctuations which exceed the no-clustering reference values by amounts comparable to those observed in the most strongly clustered exclusive channels. However, the reference value of $\langle\omega_n^2\rangle$ is quite sensitive to the multiplicity distribution at fixed topology.

(e) The fluctuation density function $M(y)$ and its integral $\langle\omega_n^2\rangle$ are well-defined quantities which are extremely sensitive to the clustering content of a set of n-body (or n-prong) data, and therefore provide stringent tests for models for describing these data.

ACKNOWLEDGMENTS

We wish to thank Dr. R. F. Peierls and Professor J. Sandweiss for several helpful conversations, and A. J. Slaughter for discussions of the reaction $K^-p \to K^-p\pi^+\pi^-\pi^0$.

APPENDIX: STATISTICAL REFERENCE MODEL

Consider a distribution $g(y)$, which may be different from the observed $p(y)$, generated by a process where energy-momentum conservation is ignored, and let each of the n rapidities be a random variable with distribution, $g(y)$, as one would assume in an independent-emission picture. The rapidities in each event form a random sample, and the distribution $\rho(z)$ obtained from a large number of such events is an n-fold convolution of $g(y)$. The Cramér test would apply to this sample, and $\langle\omega_n^2\rangle$ would be $1/6n$. The problem, then, consists of constraining this sample space by forming the appropriate conditional probability, so that the z distribution is the observed $\rho(z)$. If $g(y)$ is correctly chosen, then the distribution of rapidities on this smaller sample space will be $p(y)$, the observed rapidity distribution. In other words, we must evaluate the conditional probability

$$Q_r^\rho(y) = \int dz\, \mathcal{P}\{S_n(y) = r/n \,|\, Z = z\}\rho(z), \tag{A1}$$

where $\rho(z)$ is observed, and $S_n(y)$ is defined in Eq. (3). We follow the usual convention that upper-case letters denote random variables and lower-case letters their values. $\mathcal{P}\{A = a|B = b\}$ means the probability that $A = a$, given that $B = b$. The problem is to evaluate Eq. (A1) and use it to obtain $F(y)$, $p(y)$, and $M(y)$.

We first review the case of no constraint. Let $G(y)$ be the cumulative distribution of $g(y)$. Then $\mathcal{P}\{S_n(y) = r/n\}$ is given by the binomial distribution

$$\mathcal{P}\{S_n(y) = r/n\} = \frac{n!}{r!(n-r)!}\, G(y)^r\,[1 - G(y)]^{n-r}. \tag{A2}$$

A short calculation then gives

$$\langle S_n(y)^2\rangle = \sum_{r=0}^{n}\left(\frac{r}{n}\right)^2 \mathcal{P}\{S_n(y) = r/n\}$$

$$= [G(y)]^2 + \frac{1}{n}G(y)[1 - G(y)]. \tag{A3}$$

From Eq. (7), $\langle\omega_n^2\rangle$ is:

$$\langle\omega_n^2\rangle = \frac{1}{n}\int_0^1 dG\, G(1-G)$$

$$= 1/6n, \tag{A4}$$

as we had already stated. This also shows that the first moment of the Cramér test is distribution free. (The second moment can be gotten from a lengthier calculation, $\langle\omega_n^4\rangle = (1 - \frac{1}{3}n)/20n^2$.) For a simpler proof that ω_n^2 is distribution free, see Gibbons, Ref. 5.

Next, the conditional probability, Eq. (A1), must be computed. Although $\mathcal{P}\{S_n(y) = r/n|Z = z\}$ is difficult to compute directly, $\mathcal{P}\{Z = z\,|\,S_n(y) = r/n\}$ is easy, and is related to the former conditional probability through Bayes theorem:

$$\mathcal{P}\{S_n(y) = r/n \,|\, Z = z\}$$

$$= \frac{\mathcal{P}\{Z = z\,|\,S_n(y) = r/n\}\mathcal{P}\{S_n(y) = r/n\}}{\mathcal{P}\{Z = z\}}. \tag{A5}$$

(We use Bayes theorem in a non-Bayesian way. Equation (A5) can be trivially derived from the definition of conditional probability.) We emphasize that $\mathcal{P}\{Z = z\}$ and $\mathcal{P}\{S_n(y) = r/n\}$ are defined on the full (unconstrained) sample space, so that $\mathcal{P}\{S_n(y) = r/n\}$ is given by Eq. (A2), and $\mathcal{P}\{Z = z\}$ is an n-fold convolution of $g(y)$:

$$\mathcal{P}\{Z=z\} = g^{n*}(z)$$

$$\equiv \int \delta\left(z - \sum_{i=1}^{n} y_i\right) \prod_{i=1}^{n} [g(y_i)dy_i]. \qquad \text{(A6)}$$

$\mathcal{P}\{Z=z \mid S_n(y)=r/n\}$ is defined on the subspace where r rapidities are less than or equal to y, and $n-r$ are greater than y. According to the independent-particle-emission picture, the r rapidities on the left of y follow the left tail of $g(y)$, and the $n-r$ rapidities to the right of y follow the right tail. The (unnormalized) left- and right-tail distributions are defined, respectively, by

$$g_L(x) = \begin{cases} g(x), & x \leq y \\ 0, & x > y; \end{cases}$$
$$g_R(x) = \begin{cases} 0, & x \leq y \\ g(x), & x > y. \end{cases} \qquad \text{(A7)}$$

Since Z is a sum of *independent* random variables, and the order of the rapidities makes no difference, $\mathcal{P}\{Z=z \mid S_n(y)=r/n\}$ is simply a convolution of the left- and right-tail distributions:

$$\mathcal{P}\{Z=z \mid S_n(y)=r/n\} = \frac{g_L^{r*} * g_R^{(n-r)*}(z)}{[G(y)]^r[1-G(y)]^{n-r}}. \qquad \text{(A8)}$$

With Eqs. (A2), (A6), and (A8), Eq. (A5) becomes

$$\mathcal{P}\{S_n(y)=r/n \mid Z=z\} = \frac{n!}{r!(n-r)!} \frac{g_L^{r*} * g_R^{(n-r)*}(z)}{g^{n*}(z)}. \qquad \text{(A9)}$$

The y dependence is implicitly contained in g_L and g_R.

When working with convolutions, it is often helpful to introduce Fourier transforms:

$$\hat{g}(k) = \int_{-\infty}^{\infty} dx\, g(x) e^{ixk}, \qquad \text{(A10a)}$$

$$\hat{g}_L(k) = \int_{-\infty}^{y} dx\, g(x) e^{ixk}, \qquad \text{(A10b)}$$

$$\hat{g}_R(k) = \int_{y}^{\infty} dx\, g(x) e^{ixk}, \qquad \text{(A10c)}$$

$$\hat{g}_L(k) + \hat{g}_R(k) = \hat{g}(k). \qquad \text{(A11)}$$

After Eqs. (A10) are substituted into Eqs. (A6) and (A9), the convolutions become

$$g^{n*}(z) = \frac{1}{2\pi} \int_{-\infty}^{\infty} dk\, \hat{g}(k)^n e^{-ikz} \qquad \text{(A12a)}$$

$$g_L^{r*} * g_R^{(n-r)*}(z) = \frac{1}{2\pi} \int_{-\infty}^{\infty} dk\, \hat{g}_L(k)^r \hat{g}_R(k)^{n-r} e^{-ikz} \qquad \text{(A12b)}$$

This allows us to write the conditional probability for $S_n(y)$, Eq. (A1), in the form

$$Q_r^{\rho}(y) = \frac{n!}{r!(n-r)!} \int_{-\infty}^{\infty} dz\, \rho(z)\gamma(z) \times \int_{-\infty}^{\infty} dk\, \hat{g}_L(k)^r \hat{g}_R(k)^{n-r} e^{-ikz},$$

where

$$\gamma(z) = \left[\int_{-\infty}^{\infty} dk\, \hat{g}(k)^n e^{-ikz}\right]^{-1}. \qquad \text{(A13)}$$

Without a constraint, $\rho(z)$ would be given by the convolution Eq. (A12a), and $Q_r^{\rho}(y)$ in Eq. (A13) then reduces to Eq. (A2). In general, though, the experimentally observed $\rho(z)$ is much narrower than $g^{n*}(z)$, and Eq. (A13) is the basic equation for computing $p(y)$ and $M(y)$ in terms of $g(y)$ and $\rho(z)$. $F(y)$ is the average of $S_n(y)$:

$$F(y) = \langle S_n(y) \rangle = \sum_{r=0}^{n} \left(\frac{r}{n}\right) Q_r^{\rho}(y)$$
$$= 1 - \int_{-\infty}^{\infty} dz\, \rho(z)\gamma(z) \int_{-\infty}^{\infty} dk\, \hat{g}_R(k)\hat{g}(k)^{n-1} e^{-izk}, \qquad \text{(A14)}$$

where we have used Eq. (A11). The density $p(y)$ is simply $dF(y)/dy$:

$$p(y) = \int_{-\infty}^{\infty} dz\, \rho(z)\gamma(z) \int_{-\infty}^{\infty} dk\, \hat{g}(k)^{n-1} g(y) e^{i(y-z)k}. \qquad \text{(A15)}$$

We should emphasize that the observed distributions are $p(y)$ and $\rho(z)$. The distribution $g(y)$ is merely a construct used in formulating the problem and is not observed.

To compute $M(y)$, we must evaluate $\langle S_n(y)^2 \rangle$ which involves a sum similar to Eq. (A3). From the definition of $M(y)$, Eq. (5), the reference curve, $M_R(y)$ can be written as

$$M_R(y) = \left(\left\{\frac{1}{n} - [1-F(y)]\right\}[1-F(y)] + \frac{n-1}{n}\Delta(y)\right) p(y), \qquad \text{(A16)}$$

where

$$\Delta(y)=\int_{-\infty}^{\infty} dz\,\rho(z)\gamma(z)\int_{-\infty}^{\infty} dk\,\hat{g}_R(k)^2\,\hat{g}(k)^{n-2}\,e^{-izk}\,, \tag{A17}$$

and $F(y)$ and $p(y)$ are computed from Eqs. (A14) and (A15), respectively. The reference value $\langle\omega_n^2\rangle_{\rm ref}$ is gotten by integrating Eq. (A16) [See Eq. (7)]:

$$\langle\omega_n^2\rangle_{\rm ref}=\frac{n-1}{n}\int_{-\infty}^{\infty} dy\,p(y)\,\Delta(y)+\frac{1}{2n}-\frac{1}{3}\,. \tag{A18}$$

The reference problem is now reduced to that of finding a $g(y)$ which gives the observed $p(y)$ through Eq. (A15), and then computing a few Fourier transforms. Unfortunately, $\langle\omega_n^2\rangle_{\rm ref}$ in Eq. (A18) is no longer distribution free, so that, in principle, it is necessary to find $g(y)$ for every $p(y)$. However, $\langle\omega_n^2\rangle_{\rm ref}$ is insensitive enough to the exact shape of $p(y)$ that this presents little difficulty. Moreover, in practice, $g(y)$ and $p(y)$ are similar enough so that $g(y)$ is easily adjusted to give the desired $p(y)$.

Although Eq. (A15) is a complicated integral equation for $g(y)$ in terms of $p(y)$, it is still possible to find many useful solutions. In working with center-of-mass variables, one often has the situation where $p(y)$ and $\rho(z)$ are both approximately Gaussian. Then $g(y)$ is also a Gaussian distribution and the equations are completely soluble. This solution is presented below. In working with $k_L^{\rm lab}$, $g(y)$ given by a Poisson distribution and $\rho(z)$ arbitrary is also very manageable, since most of the integrals can be done analytically. For the sake of brevity, we will not present the Poisson solution here.

In the Gaussian model, we search for solutions to Eq. (A15) where $p(y)$ and $\rho(z)$ are Gaussian distributions centered at zero,

$$p(y)=\frac{1}{(2\pi)^{1/2}\sigma}\exp\left(-\frac{y^2}{2\sigma^2}\right), \tag{A19a}$$

$$\rho(z)=\frac{1}{(2\pi)^{1/2}w}\exp\left[-\frac{z^2}{2w^2}\right]. \tag{A19b}$$

Then $g(y)$ is also a Gaussian with zero mean and variance γ, where

$$\gamma^2=\sigma^2\frac{n^2-r^2}{n(n-1)}\,, \tag{A20a}$$

with

$$r=\frac{w}{\sigma}=\frac{\sigma_z}{\sigma_y}\,, \tag{A20b}$$

where r is the ratio of the variances of $\rho(z)$ and $p(y)$. The solution Eqs. (A20) can be checked by substituting them into Eq. (A15). [If the mean of $\rho(z)$ is not zero, and the mean of $p(y)$ is zero, then $g(y)$ is no longer Gaussian.] The Cramér limit is recovered when $r^2=n$. This solution can now be substituted into Eqs. (A16) and (A17), and $\Delta(y)$ is given by

$$\Delta(y)=\frac{1}{2\sqrt{\pi}}\int_{y/\sqrt{2}\sigma}^{\infty} dx\,e^{-x^2}\,\mathrm{erfc}\left(\alpha\frac{y}{\sqrt{2}\sigma}+\beta x\right), \tag{A21}$$

where

$$\alpha=n(n-1)[(n^2-r^2)(n^2-2n+r^2)]^{-1/2},$$

$$\beta=(n-r^2)[(n^2-r^2)(n^2-2n+r^2)]^{-1/2}, \tag{A22}$$

and

$$F(y)=1-\tfrac{1}{2}\,\mathrm{erfc}\left(\frac{y}{\sqrt{2}\sigma}\right),$$

where $\mathrm{erfc}(x)$ is the complementary error function. The reference value $\langle\omega_n^2\rangle_{\rm ref}$ is then evaluated from Eq. (A18). Table I contains some results for $n=3$ to 16.

---

*Research supported by the U. S. Atomic Energy Commission under Contract No. COO-3075.

[1]The longitudinal phase-space analysis is formulated by L. Van Hove [Nucl. Phys. B9, 331 (1969)]; some applications of this analysis relevant to our discussion here are given by J. Beaupre *et al.* [*ibid.* B35, 61 (1971)] and M. Deutschmann *et al.* [*ibid.* B50, 80 (1972)]. The prism-plot analysis is discussed by T. Brau *et al.* [Phys. Rev. Lett. 27, 1481 (1971)]. Also see J. Slaughter, Ph.D. thesis, Yale, 1973 (unpublished).

[2]W. Burdett *et al.*, Nucl. Phys. B48, 13 (1972).

[3]For a detailed description of the data analyzed in this paper see T. W. Ludlam, Ph.D. dissertation, Yale, 1969 (unpublished). An analysis of 4-body final states using the longitudinal phase-space technique for some 10-GeV/c K^-p data is given by Beaupre *et al.* (Ref. 1).

[4]H. Cramér, Skand. Aktuarietids 11, 13 (1928); 11, 141 (1928); R. von Mises, *Wahrscheinlichkeitsrechnung* (Leipzig, 1931); D. A. Darling, Ann. Math. Stat. 28, 823 (1957).

[5]J. D. Gibbons, *Nonparametric Statistical Inference* (McGraw-Hill, New York, 1971); W. T. Eadie, D. Dryard, F. E. James, M. Roos, and B. Sadoulet, *Statistical Methods in Experimental Physics* (North-Holland, Amsterdam, 1971).

[6]W. Kittel, L. Van Hove, and W. Wojcik, Computer Physics Communications 1, 425 (1970); R. F. Peierls, private communication.

[7]A sample of about 500 events ensures a statistical uncertainty in $\langle\omega_n^2\rangle$ of less than 1%.